Rapid crustal accretion and magma assimilation in the Oman-U.A.E. ophiolite: High precision U-Pb zircon geochronology of the gabbroic crust

Matthew Rioux,[1] Samuel Bowring,[1] Peter Kelemen,[2] Stacia Gordon,[3] Frank Dudás,[1] and Robert Miller[4]

Received 1 March 2012; revised 16 May 2012; accepted 22 May 2012; published 13 July 2012.

[1] New high-precision U/Pb zircon geochronology from the Oman-United Arab Emirates (U.A.E.) ophiolite provides insight into the timing and duration of magmatism and the tectonic setting during formation of the lower crust. The new data come from a well-preserved and exposed crustal section in the center of the Wadi Tayin massif. Single grain and grain fragment $^{206}Pb/^{238}U$ dates from upper-level gabbros, tonalites/trondhjemites and gabbroic pegmatites, corrected for initial Th exclusion, range from 112.55 ± 0.21 to 95.50 ± 0.17 Ma, with most data clustered between 96.40 ± 0.17 to 95.50 ± 0.17 Ma. Zircon dates from upper-level gabbros are most consistent with the ophiolite forming at a fast spreading ridge with half-rates of 50–100 km/Ma. Dates from tonalites/trondhjemites and from a gabbroic pegmatite associated with a wehrlite intrusion overlap with dates from adjacent upper-level gabbros, suggesting that any age differences between these three magmatic series are smaller than the analytical uncertainties or intrasample variability in the dates. Three of the dated upper-level gabbros and a single gabbroic pegmatite from the base of the crust have >1 Ma intrasample variability in single grain dates, suggesting assimilation of older crust during the formation or crystallization of the magmas. Whole rock $\varepsilon_{Nd}(t)$ of seven samples, including the upper-level gabbros with variable zircon dates, have tightly clustered initial values ranging from $\varepsilon_{Nd}(96\ Ma) = 7.59 \pm 0.23$ to 8.28 ± 0.31. The ε_{Nd} values are similar to those from other gabbros within the ophiolite, suggesting that any assimilated material had a similar isotopic composition to primitive basaltic magmas. The new dates suggest that the studied section formed at a fast spreading mid-ocean ridge between ~96.4–95.5 Ma. The large intrasample variability in zircon dates in some samples is unexpected in this setting, and may be related to propagation of a younger ridge into older oceanic lithosphere.

Citation: Rioux, M., S. Bowring, P. Kelemen, S. Gordon, F. Dudás, and R. Miller (2012), Rapid crustal accretion and magma assimilation in the Oman-U.A.E. ophiolite: High precision U-Pb zircon geochronology of the gabbroic crust, *J. Geophys. Res.*, *117*, B07201, doi:10.1029/2012JB009273.

1. Introduction

[2] The Oman-U.A.E. ophiolite is the largest sub-aerial exposure of oceanic lithosphere on Earth and has played a key role in our understanding of processes at oceanic spreading ridges. The exposed crust and mantle provide the opportunity to directly study lower crustal rocks that are often covered by volcanic rocks and difficult to observe and sample at modern ridges. There has been extensive research devoted to understanding the structure of the Oman-U.A.E. ophiolite crust and mantle [e.g., *Ceuleneer et al.*, 1988; *Lippard et al.*, 1986; *Nicolas et al.*, 2000a], the igneous processes active during crustal accretion [e.g., *Browning and Smewing*, 1981; *Kelemen et al.*, 1997a; *Nicolas et al.*, 1988; *Pallister and Hopson*, 1981], and the tectonic origin of the ophiolite [e.g., *Boudier et al.*, 1988; *Gray and Gregory*, 2000; *Hacker et al.*, 1996; *Pearce et al.*, 1981; *Searle and Cox*, 2002; *Searle and Malpas*, 1980]. The results from these studies have influenced current models for the structure of the oceanic lithosphere and the formation of the lower oceanic crust.

[3] Much less is known about the timing and time scales of magmatic processes within the ophiolite. Recent application of U-Pb zircon geochronology to gabbros, gabbronorites,

[1]Department of Earth, Atmospheric and Planetary Sciences, Massachusetts Institute of Technology, Cambridge, Massachusetts, USA.
[2]Lamont Doherty Earth Observatory, Columbia University, Palisades, New York, USA.
[3]Department of Geological Sciences and Engineering, University of Nevada, Reno, Nevada, USA.
[4]Geology Department, San Jose State University, San Jose, California, USA.

Corresponding author: M. Rioux, Department of Earth, Atmospheric and Planetary Sciences, Massachusetts Institute of Technology, Cambridge, MA 02459, USA. (riouxm@mit.edu)

0148-0227/12/2012JB009273

diorites, tonalites, trondhjemites and quartz diorites from the modern Mid-Atlantic Ridge, Southwest Indian Ridge and East Pacific Rise, has begun to provide insight into the chronology of magmatism within the lower crust at both slow- and fast-spreading centers [*Baines et al.*, 2009; *Grimes et al.*, 2008; *Lissenberg et al.*, 2009; *Rioux et al.*, 2012; *Schwartz et al.*, 2005]. However, there are relatively few U-Pb zircon dates from the Oman-U.A.E. ophiolite and most are from tonalites and trondhjemites [*Goodenough et al.*, 2010; *Tilton et al.*, 1981; *Warren et al.*, 2005], which form volumetrically minor intrusions into the dominantly gabbroic crust. The lower crustal exposures in the Oman-U.A.E. ophiolite provide the opportunity to expand on the research from modern ridges and to study the temporal evolution of large expanses of lower oceanic crust with well-defined structural and petrologic relationships, potentially providing new insight into both mid-ocean ridge processes and the origin of the ophiolite.

[4] Here we present a new data set of high-precision isotope dilution-thermal ionization mass spectrometry (ID-TIMS) single grain U-Pb zircon dates, from mostly gabbroic rocks within the ophiolite. Our research focused on a well-preserved and exposed lithospheric section in the Wadi Tayin massif, with the goal of studying the timescales and distribution of magmatism during crustal accretion and better constraining the spreading rate during formation of the ophiolite crust.

2. Geologic Setting and Background

[5] The analyzed samples come from the central part of the Wadi Tayin massif, which preserves a ~40 km long east–west transect perpendicular to the strike of the sheeted dikes and the inferred ridge axis (Figure 1). The area has a relatively simple structural and volcanic history and is thus one of the best places in the ophiolite to study processes of oceanic crustal accretion. This region has been interpreted as the northern limb of an east–west trending syncline, with the axis running through the exposed pillow basalts [*Hopson et al.*, 1981; *Pallister and Hopson*, 1981]. The limb dips steeply to the south exposing a full lithospheric cross section, which is traversed by multiple north–south drainages. Several north- to northwest-striking faults cut the section, but generate only kilometer-scale offsets of the mantle-crust transition and upper/lower gabbro contact (Figure 1).

[6] The mantle and crustal rocks in the study area have been described in detail by many previous workers [*Bosch et al.*, 2004; *Boudier and Coleman*, 1981; *Boudier and Nicolas*, 2011; *France et al.*, 2009; *Garrido et al.*, 2001; *Gregory and Taylor*, 1981; *Hanghøj et al.*, 2010; *Hopson et al.*, 1981; *Kelemen et al.*, 1997a; *McCulloch et al.*, 1981; *Nicolas et al.*, 2009; *Nicolas et al.*, 2000a; *Pallister*, 1981; *Pallister and Knight*, 1981; *Pallister and Hopson*, 1981; *VanTongeren et al.*, 2008] and are typical of the lithosphere seen in other parts of the ophiolite. The general crustal stratigraphy, starting at the crust-mantle transition, consists of compositionally layered gabbros; foliated gabbros; upper-level gabbros and tonalites, trondhjemites, and quartz diorites; sheeted dikes; and basaltic pillows and lavas. The layered gabbros are locally intruded by cm- to m-scale gabbroic pegmatite sills and dikes and the entire plutonic crust is locally intruded by a late wehrlite and olivine gabbro series.

[7] The volcanic rocks in this area have been assigned to the Geotimes unit and are interpreted to have been derived from MORB-like parental magmas, although they have a possible supra-subduction zone geochemical signature and a fractionation trend characterized by lower Ti and higher SiO_2 contents than typical MORB [*Alabaster et al.*, 1982; *Bibby et al.*, 2011; *Braun*, 2004; *Godard et al.*, 2003; *MacLeod et al.*, 2012; *Pallister and Knight*, 1981; *Pearce et al.*, 1981]. In general, there is little or no evidence in the Wadi Tayin massif for later, chemically distinct volcanic rocks (Alley, Lasail, clinopyroxene-phyric and Salahi units) that are found in the northern parts of the ophiolite and plutonic rocks related to these later volcanic suites (gabbronorite, pyroxenite) form only minor intrusions into mantle peridotite [*Alabaster et al.*, 1982; *Amri et al.*, 1996; *Benoit et al.*, 1996; *Hanghøj et al.*, 2010; *Kelemen et al.*, 1997b; *Pearce et al.*, 1981; *Python and Ceuleneer*, 2003; *Smewing*, 1981; *Tamura and Arai*, 2006], suggesting a simpler and shorter-lived magmatic history in this area.

[8] To relate the new U-Pb dates to the magmatic evolution of oceanic crust, it is important to understand the origin of the dated rocks. The dated samples include eight upper-level gabbros, one tonalite, one trondhjemite and two gabbroic pegmatites that intrude the layered gabbros (Figure 1 and Table 1). The upper-level gabbros are texturally heterogeneous and include medium grained isotropic gabbros, microgabbros and gabbroic pegmatites [*MacLeod and Yaouancq*, 2000], and typically contain plagioclase + clinopyroxene + Fe-Ti oxides ± amphibole ± olivine. Geochemical analyses indicate that the layered and foliated gabbros have cumulate compositions, while the upper-level gabbros have more evolved compositions that overlap the sheeted dike and lava compositions [*Garrido et al.*, 2001; *Kelemen et al.*, 1997a; *MacLeod and Yaouancq*, 2000]. Based on these data, the upper level gabbros are typically interpreted as evolved melts derived from the cumulate layered gabbros [*France et al.*, 2009; *Kelemen et al.*, 1997a; *MacLeod and Yaouancq*, 2000; *Pallister and Hopson*, 1981], and may represent the solidified remains of an axial melt lens [*MacLeod and Yaouancq*, 2000]. Alternately, the upper level gabbros have also been attributed to melting during interaction of magmatic and hydrothermal systems [*Nicolas and Boudier*, 2011; *Nicolas et al.*, 2008].

[9] Tonalites, trondhjemites and quartz diorites are found at a wide variety of structural levels within the ophiolite, from mantle to sheeted dike depths. The most common occurrence of the felsic rocks are as sills, dikes and small plutons that intrude the upper-level gabbros and the base of the sheeted dikes. The tonalite and trondhjemite dated in this study come from this structural level. These rocks have been attributed to late-stage fractionation of mafic magmas [*Amri et al.*, 1996; *Pallister and Hopson*, 1981; *Tilton et al.*, 1981] or to on-axis anatexis of hydrothermally altered gabbros [*Nicolas et al.*, 2008; *Rollinson*, 2009; *Stakes and Taylor*, 2003]. Hydrous partial melting experiments on oceanic gabbros at upper crustal pressures demonstrate that this is a viable mechanism for generating K-poor felsic magmas at mid-ocean ridges [*Koepke et al.*, 2004].

[10] The two dated gabbroic pegmatites come from the base and middle of the crust, respectively. The first sample (8111M02/9114M01A) is from a dike that cuts the layered gabbros directly above the crust-mantle transition. Similar

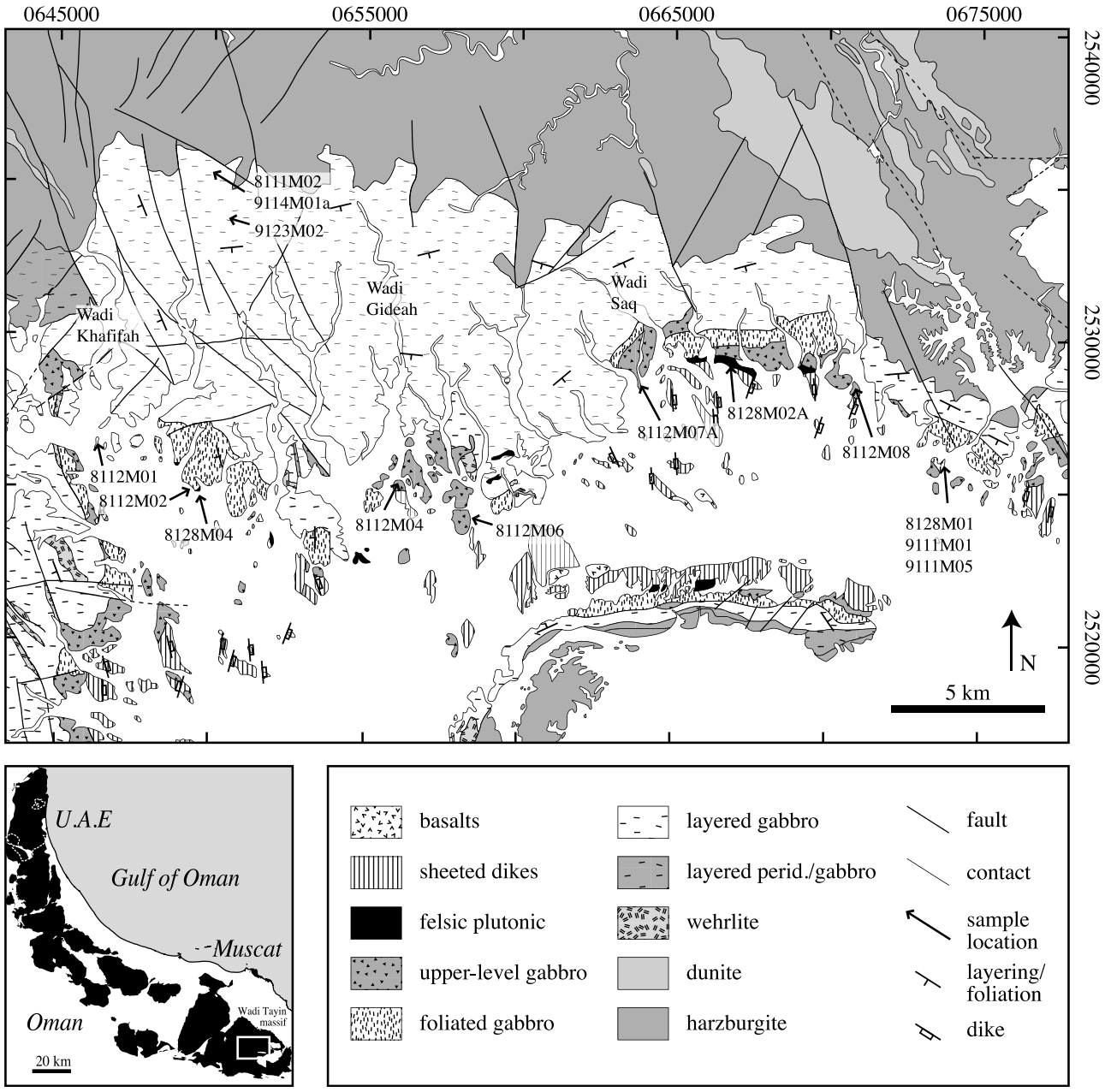

Figure 1. Geologic map of the study area in the Wadi Tayin massif near the town of Ibra (modified from *de Gramont et al.* [1986] and *El Amin et al.* [2005]). Sample locations are shown with arrows. The wehrlite unit includes wehrlite, troctolite, plagioclase-bearing dunite, and olivine pyroxenite. Numbers along the axes are UTM coordinates. Representative layering, foliation and sheeted dike orientations are shown (tick in the downdip direction). Location map in the bottom left corner shows the extent of ophiolite-related rocks in eastern Oman and the United Arab Emirates (U.A.E.) (modified from *Nicolas et al.* [2000a]). White rectangle on the ophiolite map shows the study area enlarged in the main map. White dashed lines are the Oman-U.A.E. borders.

veins and dikes throughout the crust have been attributed to either evolved melts expelled from the cumulate layered gabbros [*Lippard et al.*, 1986; *Pallister and Hopson*, 1981] or hydrous melting due to deep penetration of hydrothermal fluids near the ridge axis [*Bosch et al.*, 2004; *Nicolas et al.*, 2000b]. The second dated pegmatite (9123M02) is associated with a wehrlite body, and field relations suggest that similar wehrlite magma series throughout the ophiolite were intruded prior to complete solidification of the lower crust [*Juteau et al.*, 1988; *Pallister and Hopson*, 1981].

3. Existing Geochronology

[11] Several prior studies have used U-Pb zircon and K-Ar or ^{40}Ar-^{39}Ar dating to constrain the crystallization and cooling history of the ophiolite [*Gnos and Peters*, 1993;

Table 1. Sample Locations and Descriptions

Sample	UTM (E)[a]	UTM (N)[a]	Rock Type	Mineralogy[b]
8111 M02	0650157	2535313	gabbroic pegmatite	pl + cp + ol + am
8112 M01	0646354	2526483	gabbro	pl + cp + ox + (am)
8112 M02	0649506	2524855	gabbro	pl + cp + am + ox
8112 M04	0656229	2525209	gabbro	pl + cp + ox + (am)
8112 M06	0658471	2524011	gabbro	pl + cp + am + ox
8112M07A	0664156	2528741	gabbro	pl + cp + ox
8112 M08	0671047	2528340	gabbro	pl + cp + am + ox
8128 M01	0673902	2526033	gabbro	pl + cp + ox
8128M02A	0666939	2529113	trondhjemite	pl + qt + ox + am
8128 M04	0649597	2524808	tonalite	pl + qt + ox + am
9111 M01	0673815	2525930	gabbro	pl + cp + am + ox
9111 M05	0673902	2526035	gabbro	pl + cp + ox + am
9114M01A	0650155	2535307	gabbroic pegmatite	pl + cp + ol + am
9123 M02	0650634	2533667	gabbroic pegmatite	pl + cp + am + ox

[a]WGS 84.

[b]pl, plagioclase; cp, clinopyroxene; ol, olivine; am, amphibole; ox, oxide; qt, quartz; parentheses denote secondary minerals.

Goodenough et al., 2010; *Hacker*, 1994; *Hacker et al.*, 1996; *Lanphere*, 1981; *Montigny et al.*, 1988; *Searle et al.*, 1980; *Tilton et al.*, 1981; *Warren et al.*, 2005]. In a pioneering study, *Tilton et al.* [1981] dated thirteen large multigrain zircon fractions (~10 mg each) from felsic plutonic samples collected throughout the ophiolite. The $^{206}Pb/^{238}U$ dates range from 97.3 ± 0.4 to 93.5 ± 0.4 Ma with most concentrated around 95 Ma (2σ uncertainties). More recent analyses of small multigrain fractions (2–9 grains) from four of the same sample locations yielded $^{206}Pb/^{238}U$ dates from 96.02 ± 0.67 to 94.18 ± 0.54 Ma [*Warren et al.*, 2005]—within error but slightly older than the *Tilton et al.* [1981] dates. *Goodenough et al.* [2010] studied a later magmatic series that intrudes the main crustal section in ophiolite massifs within the U.A.E. and reported ID-TIMS U-Pb zircon $^{206}Pb/^{238}U$ dates of 95.76 ± 0.48 to 95.22 ± 0.37 Ma on small multigrain fractions (7–42 μg) from tonalite and gabbro samples (all reported dates are fraction dates; the reported *Warren et al.* [2005] and *Tilton et al.* [1981] dates have been Th-corrected using the same Th/U of the magma as we used to correct our analyses; *Goodenough et al.* [2010] did not report the parameters necessary to recalculate the data and we report the published uncorrected values, excluding analyses with 2σ uncertainties > 1 Ma). These published U-Pb dates provide the only quantitative constraints on crystallization ages within the ophiolite.

[12] ^{40}Ar-^{39}Ar data provide insight into the cooling history of the lithosphere and underlying metamorphic sole. Hornblende ^{40}Ar-^{39}Ar data from gabbros, tonalites/trondhjemites and hornblende veins record dates of 98.4 ± 2.6/4.7 to 95.3 ± 1.0/3.9 Ma and are interpreted to reflect post-magmatic cooling below hornblende closure temperatures of ~550°C [*Hacker*, 1994; *Hacker et al.*, 1996]; all ^{40}Ar-^{39}Ar dates are recalculated using the *Kuiper et al.* [2008] Fish Canyon sanidine date of 28.201 ± 0.046 Ma, the decay constant ($\lambda_{tot.} = 5.463 \pm 0.214 \times 10^{-10}$ yr^{-1}) recommended by *Min et al.* [2000] and the *Renne et al.* [1998] intercalibration between the Fish Canyon sanidine and Taylor Creek sanidine; 2σ uncertainties are reported as analytical + standard/analytical + standard + decay constant. Hornblende cooling dates from the metamorphic sole—mostly from the Wadi Sumeinia and Wadi Tayin exposures—range from 98.3 ± 1.0/4.0 to 94.6 ± 1.2/3.9 Ma and the sole is cut by a mafic dike with a date of 95.7 ± 1.6/4.1 Ma [*Hacker*, 1994; *Hacker et al.*, 1996]. These data are interpreted to date rapid thrusting of the ophiolite over adjacent oceanic lithosphere, immediately following the formation of the igneous crust.

4. Results

[13] U-Pb zircon data are plotted in Figures 2 and 3 and the analytical methods (Text S1) and U-Pb data (Table S1) are included in the auxiliary material.[1] Single grains or grain fragments were analyzed by ID-TIMS using the chemical abrasion method [*Mattinson*, 2005], which minimizes or eliminates the impact of Pb-loss for the analyzed grains. Single grain $^{206}Pb/^{238}U$ dates from all 13 samples range from 112.55 ± 0.21 to 95.50 ± 0.17 Ma, with a preponderance of the dates falling in a very narrow range from 96.40 ± 0.17 to 95.50 ± 0.17 Ma. Reported uncertainties are 2σ analytical, and tracer (http://www.earth-time.org) and decay constant (^{238}U λ 2σ = ±0.107 yr^{-1}) [*Jaffey et al.*, 1971] uncertainties should be added when comparing the dates to dates measured with different tracers or isotopic systems (e.g., $^{40}Ar/^{39}Ar$). All dates discussed herein are Th-corrected (Text S1). The U-Pb zircon data fall into four distinct groups, defined by the relative dispersion of the dates within each sample:

[14] Group I: Two tonalite and trondhjemite plutons (8128M02A, 8128M04) and a single upper-level gabbro (9111M01) have single grain $^{206}Pb/^{238}U$ dates that overlap within analytical uncertainty. $^{206}Pb/^{238}U$ dates range from 96.10 ± 0.22 to 95.79 ± 0.15 Ma. Mean square of the weighted deviates (MSWD) of the weighted mean for these samples (all <1.4) are consistent with the null hypothesis that the data represent repeat measurements of a single crystallization age [*Wendt and Carl*, 1991]. The tonalite and trondhjemite samples have relatively large uncertainties, which may conceal the type of intrasample variability seen in the Group II samples.

[15] Group II: Three upper-level gabbros (8112M01, 8112M08, 9111M05) have clusters of data with no clear outliers, but two-sided p-values for the chi-square goodness of fit of <0.05 (i.e., MSWD ≫ 1), suggesting that the data do not reflect repeat measurements of a single population and that zircon crystallized over an extended interval. $^{206}Pb/^{238}U$ dates range from 96.08 ± 0.10 to 95.865 ± 0.056 Ma and the intrasample variability in single grain dates range from 0.15 ± 0.12 Ma to 0.18 ± 0.15 Ma; the intrasample variability was calculated as the difference between the maximum and minimum dates in a sample with the uncertainty equal to the sum of the uncertainties on the two dates. For samples where there is more than one analysis close to the maximum or minimum date, we used the date with the lowest uncertainties to calculate the variability.

[16] Group III: One upper-level gabbro (8112M02) and two gabbroic pegmatites that intrude the layered gabbros (9114M01A, 9123M02) have clusters of younger dates and one resolvable outlier that is ~0.1–0.3 Ma older. The

[1]Auxiliary materials are available in the HTML. doi:10.1029/2012JB009273.

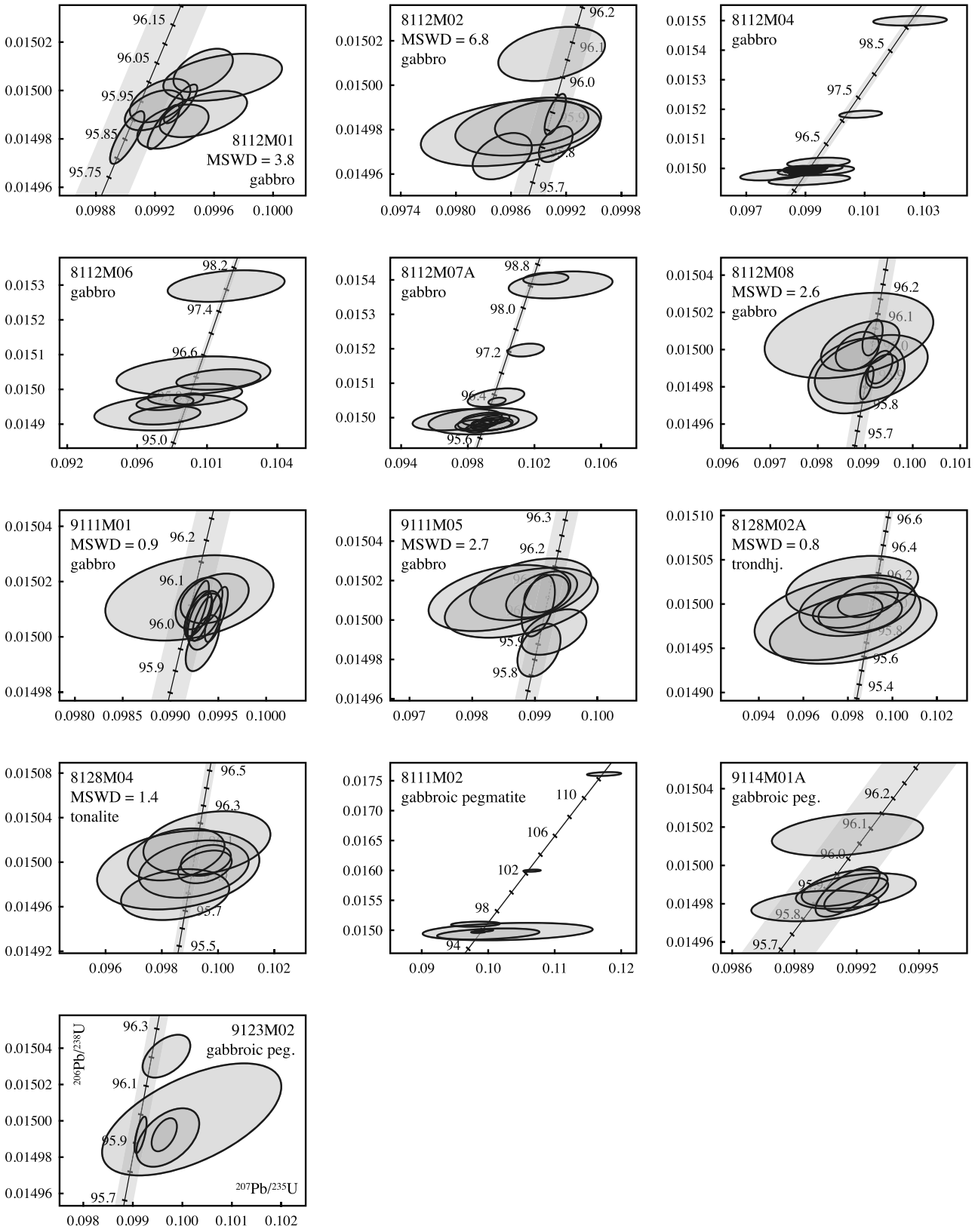
8112M01
MSWD = 3.8
gabbro
8112M02
MSWD = 6.8
gabbro
8112M04
gabbro
8112M06
gabbro
8112M07A
gabbro
8112M08
MSWD = 2.6
gabbro
9111M01
MSWD = 0.9
gabbro
9111M05
MSWD = 2.7
gabbro
8128M02A
MSWD = 0.8
trondhj.
8128M04
MSWD = 1.4
tonalite
8111M02
gabbroic pegmatite
9114M01A
gabbroic peg.
9123M02
gabbroic peg.
$^{206}Pb/^{238}U$
$^{207}Pb/^{235}U$

Figure 2

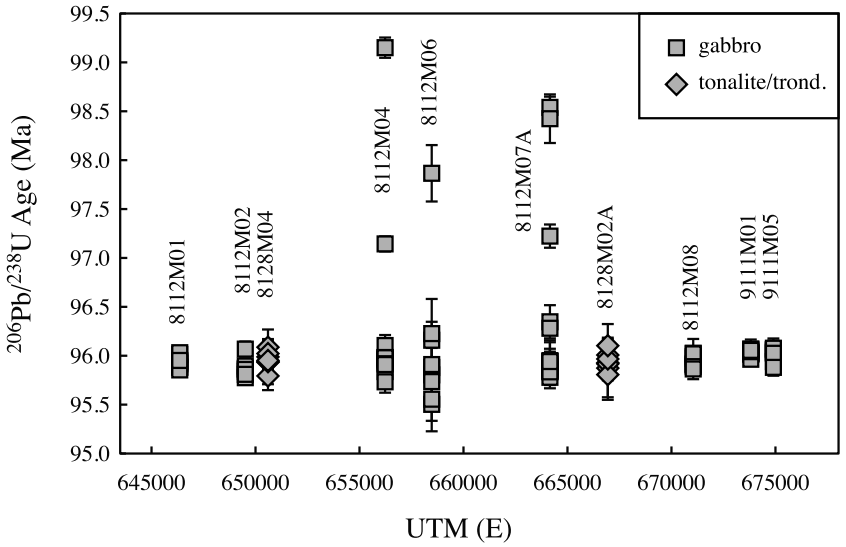

Figure 3. $^{206}Pb/^{238}U$ zircon dates (Th-corrected) versus UTM easting of upper-level gabbros, tonalite and trondhjemite. Pegmatitic samples from lower in the crust are not plotted. The *x* axis covers the same E–W distance as Figure 1. Sample 8128M04 and 9111M05 are shifted 1 km to the east for clarity.

$^{206}Pb/^{238}U$ dates in the younger clusters range from 95.93 ± 0.06 to 95.78 ± 0.07 Ma and the older outliers have dates of 96.07 ± 0.08 Ma to 96.19 ± 0.08 Ma. The total intrasample variability in single grain dates range from 0.20 ± 0.13 Ma to 0.29 ± 0.14 Ma.

[17] Group IV: Three upper-level gabbros (8112M04, 8112 M06, 8112M07A) and one gabbroic pegmatite that intrudes the layered gabbros (8111M02; same pegmatite as 9114M01A) have clusters of younger dates and one or more >1 Ma older outlier. The $^{206}Pb/^{238}U$ dates in the younger clusters range from 96.40 ± 0.17 to 95.50 ± 0.17 Ma. In the three upper-level gabbros, the oldest outliers have dates of 99.15 ± 0.10 Ma, 97.87 ± 0.29 Ma and 98.54 ± 0.11 Ma, respectively, and are 2.36 ± 0.46 Ma to 3.42 ± 0.21 Ma older than the youngest grains in each sample. In the deep crustal pegmatite, the older outliers have dates of 102.30 ± 0.11 Ma and 112.55 ± 0.21 Ma and are 6.51 ± 0.21 to 16.76 ± 0.30 Ma older than the youngest precisely dated grain.

[18] Sm-Nd isotopic analyses from seven upper-level gabbros and a trondhjemite have tightly clustered initial values ranging from ε_{Nd}(96 Ma) = 7.59 ± 0.23 to 8.28 ± 0.31 (2σ; Figure 4 and Table S2). The new data are similar to previous Nd isotopic data from the ophiolite, which include analyses from ultramafic to felsic plutonic rocks, sheeted dikes and lavas, and range from ε_{Nd}(96 Ma) = 6.08–10.22 (data re-calculated to be consistent with the fractionation correction used in this study) [*Benoit et al.*, 1996; *Godard et al.*, 2006; *McCulloch et al.*, 1981]. The data also overlap the range of values observed in in situ MORB from the Atlantic and Indian Oceans [e.g., *Hofmann*, 2007].

5. Discussion

5.1. Interpretation of the U-Pb Data

[19] The cluster of younger dates in each sample, and the similar age of the youngest grains, suggest that these dates reflect crystallization of the gabbros, tonalite, trondhjemite and pegmatites between ~96.2–95.5 Ma (Figures 2 and 3). The intrasample variability, in excess of the analytical uncertainties, in groups II and III may reflect protracted zircon crystallization in magma chambers or mush zones due to slow cooling and magma recharge, assimilation of slightly older zircons from adjacent wall rocks, and/or mixing between significantly older (>1 Ma), cryptic, inherited cores and younger magmatic rims. In the latter scenario, even the youngest dates in each sample could be older than the true crystallization age of the sample, however, we consider this unlikely because of the overlap of multiple dates in most samples and the dearth of observable cores in cathodoluminescence (CL) images (Figure S1). The >1 Ma older zircons in three upper-level gabbros and a gabbroic pegmatite (Groups IV) are interpreted as xenocrystic grains incorporated from an older source. The similar initial Nd isotopic values from many of the dated upper-level gabbros and the dated trondhjemite, including the upper-level gabbros with

Figure 2. U-Pb concordia diagrams of single-grain dates. All data are corrected for initial Th exclusion. Ages on concordia are in Ma. Grey bands represent 2σ uncertainties on concordia based on decay constant uncertainties of 0.107% (^{238}U) and 0.136% (^{235}U) [*Jaffey et al.*, 1971]. Axis labels are shown in bottom left plot. Plots and mean square of the weighted deviates (MSWD) of the weighted mean were generated using the U-Pb_redux software package [*Bowring et al.*, 2011; *McLean et al.*, 2011]. Analyses with large uncertainties relative to the other dated grains were excluded from the plots for 9111M05 (z11) and 9114M01A (z5, z9A) in all figures for clarity.

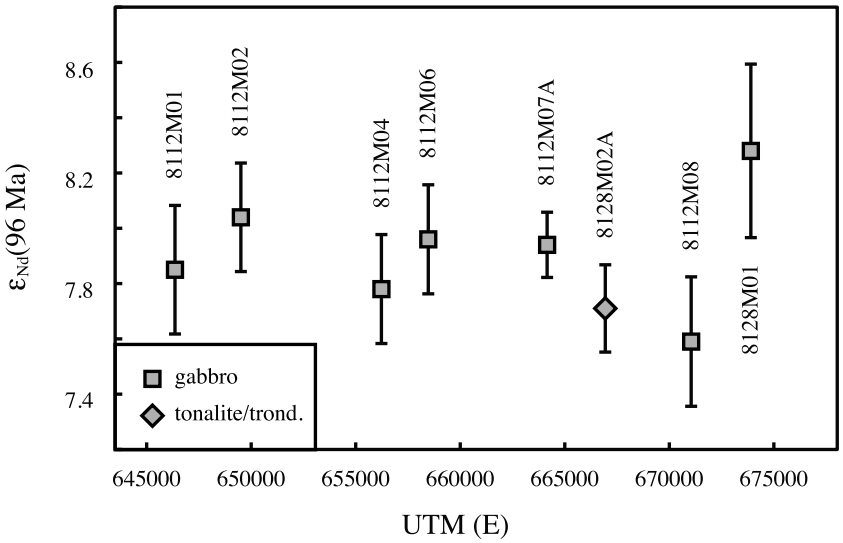

Figure 4. ε_{Nd}(96 Ma) versus UTM easting of upper-level gabbros and a trondhjemite.

xenocrystic zircons, suggest that any assimilated material had a similar isotopic composition to primitive basaltic magmas.

[20] The published U-Pb dates from *Warren et al.* [2005] (96.02 ± 0.67 to 94.18 ± 0.54 Ma) and *Goodenough et al.* [2010] (95.76 ± 0.48 to 95.22 ± 0.37 Ma) overlap with the preponderance of dates from this study (96.40 ± 0.17 to 95.50 ± 0.17 Ma), but the Warren *et al.* results extend to younger dates. The two earlier studies were carried out prior to the widespread adoption of the chemical abrasion method [*Mattinson*, 2005] and the dates are therefore more likely to reflect post-crystallization Pb-loss. The younger dates could therefore reflect true variations in crystallization ages between the different study areas or Pb-loss in some of the analyzed zircons. It is not possible to directly compare the U-Pb dates to published K-Ar or ^{40}Ar-^{39}Ar dates from the ophiolite due to uncertainties in the ^{40}K decay constant and the absolute age of ^{40}Ar-^{39}Ar mineral standards.

5.2. Relative Timing of Mafic and Felsic Magmatism

[21] The new dates constrain the timing of the gabbroic, tonalitic/trondhjemitic and late werhlitic/olivine gabbro magma series during crustal growth. Data from the two dated tonalite and trondhjemite plutons each define a single population that is within uncertainty of dates from adjacent gabbros. The agreement between the tonalite, trondhjemite and gabbro dates indicates that mafic and felsic magmas were coeval, at the resolution of our analytical uncertainties, and both likely formed during crustal accretion at a spreading-ridge axis. To constrain the timing of the late wehrlite and olivine gabbro intrusions, we dated a pegmatitic gabbro dike that intrudes layered gabbro ~1.5 km above the crust-mantle transition. Additional pegmatite intrusions from the same outcrop crosscut a wehrlite body, suggesting that the pegmatites are coeval with or younger than the wehrlite. The pegmatite data are within uncertainty of the dates from the two closest upper-level gabbro samples (8112M02, 8112M04), suggesting that the age difference between the wehrlite and upper-level gabbros is also smaller than the analytical uncertainties or intrasample variability in single grain dates.

5.3. Spreading Rate

[22] Knowledge of the spreading rate is important for understanding how observations from the ophiolite can be extrapolated to active ridges. The exposed crust in the ophiolite is interpreted to have formed at a fast-spreading ridge based on the limited range in the original U-Pb dates [*Tilton et al.*, 1981], the continuity of the layered gabbro unit [*Nicolas*, 1989; *Nicolas et al.*, 1996], and the absence of recognizable transform faults [*MacLeod and Rothery*, 1992; *Nicolas*, 1989; *Peacock*, 1990]. The *Tilton et al.* [1981] U-Pb dates provide the most quantitative constraint on the spreading rate, but the dated samples are from felsic intrusions into gabbroic rocks in multiple massifs with complex structural histories and potentially large off-sets or rotations between them, which complicate interpretation of the data.

[23] The dated samples from this study are from a ~30 km transect perpendicular to the regional strike of the sheeted dikes within a single ophiolite block, providing an ideal opportunity to constrain the spreading rate during accretion. To determine the spreading rate, we used dates from the upper-level gabbros, tonalite and trondhjemite, which all come from the same structural level directly below the sheeted dike complex. The location of the paleo-ridge axis, with respect to the dated samples, is not definitively known and we present two possible geometries (Figure 5). The simplest model assumes that the ridge axis was located to the west of the dated samples (Figure 5a), consistent with an inferred ridge axis on the western side of the Wadi Tayin massif based on sheeted dike orientations, shear sense indicators in mantle peridotites, the orientations of foliated gabbros, and mapped mantle diapirs [*Nicolas et al.*, 2000a]. If the ridge axis was instead located to the east of the transect the geometry would be reversed [*Ildefonse et al.*, 1993; *Nicolas et al.*, 2000a]. Alternately, if the youngest date in each sample is taken as the final crystallization age, the U-Pb dates from this study suggest that the paleo-ridge axis may be preserved near the center of the study area, with samples growing increasingly older to the east and west (Figure 5b). We note that the two youngest dates in sample 8112M06

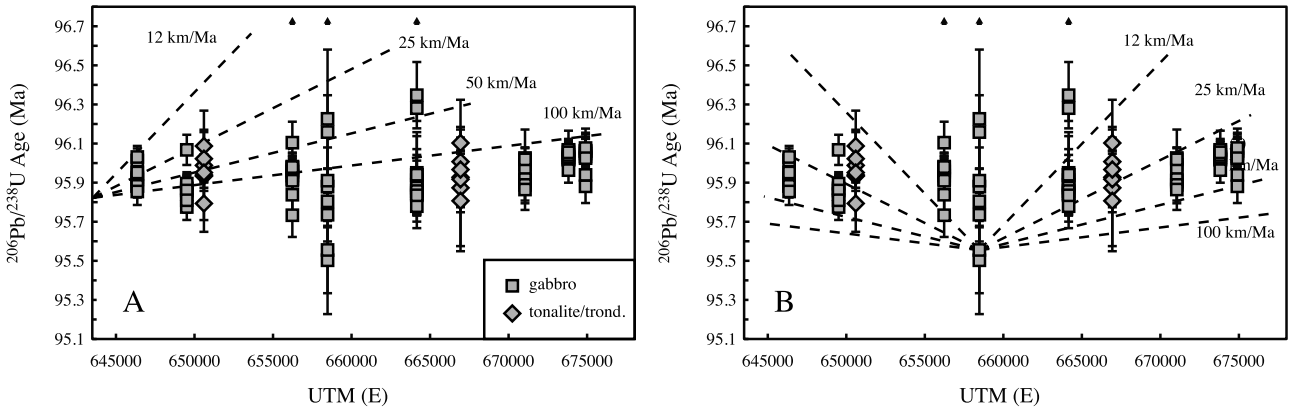

Figure 5. Comparison of different half-spreading rates to the U-Pb zircon dates from upper-level gabbros, tonalite and trondhjemite. Pegmatitic samples from lower in the crust are not plotted. (a) Model half-spreading rates assuming that the ridge axis was located to the west of the dated samples. (b) Model half-spreading rates assuming the paleo-ridge axis is preserved near the center of the study area. Older grains from samples 8112M04, 8112M06 and 8112M07A plot off the scale of the *y* axis (denoted by arrows). Sample 8128M04 and 9111M05 are shifted 1 km to the east for clarity. The data are most consistent with spreading rates of 50–100 km/Ma in each model.

have large uncertainties, but even excluding these points the youngest dates occur around Wadi Gideah. This interpretation is consistent with a change in the foliation of the layered gabbros across Wadi Gideah [*Nicolas et al.*, 2000a].

[24] It is not possible to calculate an exact spreading rate due to the dispersion of single grain dates within each sample. However, in each geometry the data are most consistent with fast to super-fast half-spreading rates of 50–100 km/Ma (Figure 5). This represents the best available constraint on the spreading rate during accretion of the Oman-U.A.E. ophiolite crust.

5.4. Comparison to Modern Ridges

[25] Recent studies have reported U-Pb zircon dates from plutonic crust formed at the slow-spreading Mid-Atlantic Ridge and Southwest Indian Ridge and the fast-spreading East Pacific Rise [*Baines et al.*, 2009; *Grimes et al.*, 2008; *Lissenberg et al.*, 2009; *Rioux et al.*, 2012; *Schwartz et al.*, 2005]. These data provide the opportunity to compare the timescales of crystallization in the ophiolite and modern ridges. Three studies provide particular insight: *Schwartz et al.* [2005] presented sensitive high-resolution ion microprobe (SHRIMP) U/Pb zircon dates from the Atlantis Bank on the Southwest Indian Ridge. U/Pb dates within most samples overlapped within analytical uncertainties. However, a single evolved gabbro contained four zircons with cores that were up to 1.1 $\pm$ 0.6 Ma older than the corresponding rims (2σ; an additional lower precision core date was 1.4 $\pm$ 1.2 Ma older); the older cores were attributed to assimilation of zircons from earlier gabbros that crystallized in the mantle and were then transported into the crust. Two subsequent studies have addressed the timescales of magmatic processes at the Mid-Atlantic Ridge and the East Pacific Rise using high precision ID-TIMS U/Pb zircon dating [*Lissenberg et al.*, 2009; *Rioux et al.*, 2012]. In each area, single grain analyses in a subset of the studied samples had weighted mean MSWDs that were higher than expected for repeat measurements of a single population. Maximum likelihood estimates of the intrasample variability in ^{206}Pb/^{238}U dates from these samples range from 0.068 to 0.166 Ma for the Mid-Atlantic Ridge and 0.047–0.124 Ma for the East Pacific Rise, consistent with protracted zircon crystallization at both slow- and fast-spreading ridges.

[26] The range of dates in the Group II and III samples from this study (0.15 $\pm$ 0.12 Ma to 0.29 $\pm$ 0.14 Ma) are comparable to the intrasample variability in high precision single grain dates from the Mid-Atlantic Ridge and East Pacific Rise. In addition, the xenocrystic zircons in three upper level gabbros are consistent with the inherited cores in zircons from the Atlantis Bank. However, the range of dates in the Oman gabbros that contain xenocrystic zircons (2.36 $\pm$ 0.46 Ma to 3.42 $\pm$ 0.21 Ma) are much greater than that observed at the slow-spreading Atlantis Bank (1.1 $\pm$ 0.6 Ma). Assimilation of older zircons is also less likely to occur during normal spreading at a fast-spreading ridge because, 1) fast-spreading ridges are inferred to be characterized by a thin thermal boundary layer in the shallow mantle [e.g., *Braun et al.*, 2000; *Reid and Jackson*, 1981; *Sleep*, 1975], which inhibits gabbro crystallization at depth, and 2) material is rapidly transported away from the ridge axis, limiting the potential for interaction between magmas and older wall rocks; the 1–3 Ma dispersion in the U-Pb dates from the upper-level gabbros corresponds to 50–150 km of spreading at 50 km/Ma. We instead interpret the xenocrystic zircons to result from the tectonic setting during formation of the ophiolite crust.

5.5. Tectonic Models

[27] The simplest explanation of the new dates is that the preserved lithosphere formed by processes typical of mid-ocean ridge spreading centers [e.g., *Nicolas and Boudier*, 2003], in either an ocean basin (Figure 6a) or a supra-subduction zone setting (Figure 6b). In this case, the xenocrystic zircons may result from propagation of a younger magmatic segment into slightly older oceanic crust. There is ample evidence for ridge propagation during ophiolite

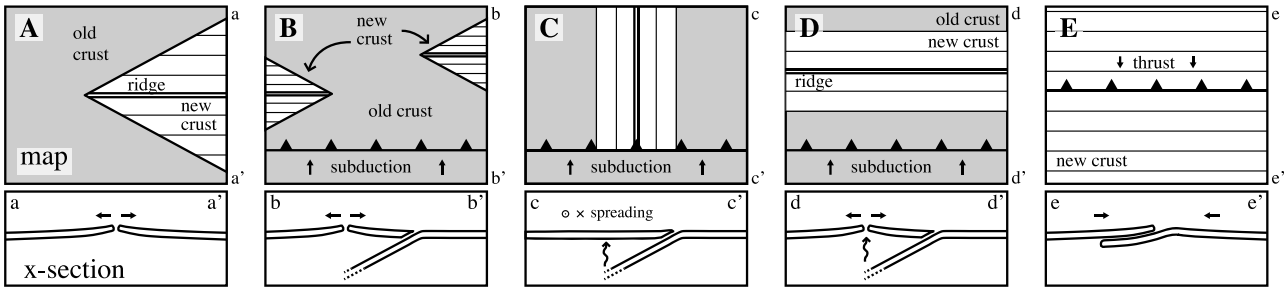

Figure 6. Tectonic models for the origin of xenocrystic zircons during formation and emplacement of the ophiolite in map view and cross section. (a) Propagation of a younger ridge into older oceanic crust at a mid-ocean ridge spreading center [e.g., *Boudier et al.*, 1997]. (b) Propagation of one or more ridges into older oceanic lithosphere above a subduction zone [*MacLeod et al.*, 2012]. (c and d) Formation of the ophiolite crust in a supra-subduction zone setting [e.g., *Dewey and Casey*, 2011; *Searle and Cox*, 1999] with material transferred from the downgoing slab to the over-riding plate. (e) Initial emplacement of the ophiolite by intraoceanic thrusting [e.g., *Boudier and Nicolas*, 2007] with transfer of material from the under-thrust to over-thrust plate.

magmatism [*Adachi and Miyashita*, 2003; *Girardeau et al.*, 2002a, 2002b; *Miyashita et al.*, 2003; *Nicolas and Boudier*, 1995; *Nicolas et al.*, 2000a; *Reuber et al.*, 1991]. This includes evidence in the Sumail massif, adjacent to the Wadi Tayin massif, for propagation of a new ridge or diapir into older lithosphere [*Amri et al.*, 1996; *Boudier et al.*, 1997; *Ceuleneer et al.*, 1996; *Godard et al.*, 2000] and off-axis, polyphase magmatism [*Jousselin and Nicolas*, 2000]. In the Wadi Tayin massif, the Makhibiyah shear zone [*Homburg et al.*, 2010; *Nicolas and Boudier*, 2008] and the large scale rotation of sheeted dike orientations from N-S in the east to NW-SE in the west [*Bailey*, 1981; *Nicolas et al.*, 2000a] could also result from plate reorganization. The abundance of propagating rifts in the geologic record of the ophiolite and paleomagnetic evidence for rotations between the different massifs have been attributed to plate rotations prior to the onset of intraoceanic thrusting and ophiolite emplacement [*Boudier et al.*, 1997; *Luyendyk and Day*, 1982; *Luyendyk et al.*, 1982; *Nicolas et al.*, 2000a; *Perrin et al.*, 1994, 2000; *Weiler*, 2000].

[28] An alternative model is that the xenocrystic zircons were derived from material thrust under the ophiolite either as a result of formation in a supra-subduction zone (Figures 6c and 6d) [*Alabaster et al.*, 1982; *Pearce et al.*, 1981; *Searle and Cox*, 2002; *Searle and Malpas*, 1980; *Warren et al.*, 2005] or during initial emplacement of the ophiolite over adjacent oceanic crust (Figure 6e) [*Boudier and Coleman*, 1981; *Boudier and Nicolas*, 2007; *Boudier et al.*, 1988; *Gregory et al.*, 1998; *Hacker*, 1991; *Hacker et al.*, 1996]. This would require that the thrusting or subduction was synchronous or very rapidly followed ridge spreading. The xenocrystic grains could be derived from either older oceanic lithosphere or sediments within the under thrust plate. In both scenarios, the xenocrystic zircons would be transported in magmas through the upper-most mantle and the entire crust of the over-riding plate to below the gabbro-sheeted dike transition. However, the magmas that formed the lavas and cumulate gabbros in the Wadi Tayin and adjacent Sumail massifs were primitive basalts with estimated magmatic temperatures of $\sim$1240 $\pm$ 20°C [*Kelemen and Aharonov*, 1998]. Zircon-saturation experiments indicate that xenocrystic zircons would rapidly ($\ll$0.1 Ma) dissolve in basaltic magmas at such high temperatures [*Harrison and Watson*, 1983]. Some upper-level gabbros could represent lower-temperature magmas that did not interact with the high-temperature magmas. However, the overall structure of the ophiolite, the consistency of initial $^{143}Nd/^{144}Nd$, and the similar crystallization ages from the studied gabbros, suggest that upper and lower gabbros in the Wadi Tayin massif were derived from a common, primitive basaltic parental magma, with little or no assimilation of, or mixing with, more isotopically evolved crustal material.

[29] We therefore prefer the interpretation that the xenocrystic zircons in the upper-level gabbros are related to assimilation of older rocks during ridge propagation. Xenocrystic zircons in the single gabbroic pegmatite from the base of the crust are significantly older (>102 Ma) than the xenocrystic grains in the upper-level gabbros and are likely related to an alternate processes, such as ophiolite emplacement.

6. Conclusion

[30] New U-Pb zircon dates from a well-preserved and exposed crustal section in the Wadi Tayin massif record a complex magmatic history. Single grain $^{206}Pb/^{238}U$ dates range from 112.55 $\pm$ 0.21 to 95.50 $\pm$ 0.17 Ma (2σ analytical; Th corrected), with most dates between 96.40 $\pm$ 0.17 to 95.50 $\pm$ 0.17 Ma. Dates from upper-level gabbros along a 30-km transect perpendicular to the regional trend of the sheeted dikes are most-consistent with the crust forming at a fast- to super-fast-spreading ridge with a half rate of 50–100 km/Ma. U-Pb dates from a gabbroic pegmatite associated with a wehrlite intrusion and two tonalites/trondhjemites from directly below the sheeted dikes are within uncertainty of dates from the nearest gabbros, suggesting that any age differences between these magmatic series are smaller than the analytical uncertainties and intrasample variations in single grain dates. Three upper-level gabbros contain xenocrystic zircons that are >1 Ma older than the youngest grains in each sample. Whole rock $\varepsilon_{Nd}(t)$ from these gabbros are similar to other gabbros from the ophiolite, suggesting that the assimilated material had a

similar isotopic composition to mid-ocean ridge gabbros. The most likely explanation for the origin of the xenocrystic zircons is that they were derived from older oceanic crust intruded by a younger, propagating ridge segment.

[31] **Acknowledgments.** We thank Adolphe Nicolas, Françoise Boudier, Brad Hacker and Chris MacLeod for useful discussions on the geology of the Oman-U.A.E. ophiolite and the data presented herein. We thank Jessica Creveling and Linnea Koons for separating zircons from many of the dated samples. Finally, we thank the Ministry of Commerce and Industry, Directorate General of Minerals in Oman for helping to facilitate our fieldwork within the ophiolite. This research was funded by NSF grant OCE-0727914.

References

Adachi, Y., and S. Miyashita (2003), Geology and petrology of the plutonic complexes in the Wadi Fizh area: Multiple magmatic events and segment structure in the northern Oman ophiolite, *Geochem. Geophys. Geosyst.*, *4*(9), 8619, doi:10.1029/2001GC000272.

Alabaster, T., J. A. Pearce, and J. Malpas (1982), The volcanic stratigraphy and petrogenesis of the Oman ophiolite complex, *Contrib. Mineral. Petrol.*, *81*(3), 168–183, doi:10.1007/BF00371294.

Amri, I., M. Benoit, and G. Ceuleneer (1996), Tectonic setting for the genesis of oceanic plagiogranites: Evidence from a paleo-spreading structure in the Oman ophiolite, *Earth Planet. Sci. Lett.*, *139*(1–2), 177–194, doi:10.1016/0012-821X(95)00233-3.

Bailey, E. H. (1981), Geologic map of Muscat-Ibra area, Sultanate of Oman, *J. Geophys. Res.*, *86*(B4), map.

Baines, A. G., M. J. Cheadle, B. E. John, C. B. Grimes, J. J. Schwartz, and J. L. Wooden (2009), SHRIMP Pb/U zircon ages constrain gabbroic crustal accretion at Atlantis Bank on the ultraslow-spreading Southwest Indian Ridge, *Earth Planet. Sci. Lett.*, *287*, 540–550, doi:10.1016/j.epsl.2009.09.002.

Benoit, M., M. Polvé, and G. Ceuleneer (1996), Trace element and isotopic characterization of mafic cumulates in a fossil mantle diapir (Oman ophiolite), *Chem. Geol.*, *134*(1–3), 199–214, doi:10.1016/S0009-2541(96)00087-3.

Bibby, L. E., C. J. MacLeod, and C. J. Lissenberg (2011), OmanDB: The role of water in axial lavas and dykes from the Oman ophiolite and geochemical segmentation of the palaeo-spreading ridge, Abstract OS11B-1485 presented at 2011 Fall Meeting, AGU, San Francisco, Calif., 5–9 Dec.

Bosch, D., M. Jamais, F. Boudier, A. Nicolas, J. M. Dautria, and P. Agrinier (2004), Deep and high-temperature hydrothermal circulation in the Oman ophiolite—Petrological and isotopic evidence, *J. Petrol.*, *45*(6), 1181–1208, doi:10.1093/petrology/egh010.

Boudier, F., and R. G. Coleman (1981), Cross section through the peridotite in the Samail ophiolite, southeastern Oman Mountains, *J. Geophys. Res.*, *86*(B4), 2573–2592, doi:10.1029/JB086iB04p02573.

Boudier, F., and A. Nicolas (2007), Comment on "dating the geologic history of Oman's Semail ophiolite: Insights from U–Pb geochronology" by C. J. Warren, R. R. Parrish, D. J. Waters and M. P. Searle, *Contrib. Mineral. Petrol.*, *154*(1), 111–113, doi:10.1007/s00410-007-0189-5.

Boudier, F., and A. Nicolas (2011), Axial melt lenses at oceanic ridges—A case study in the Oman ophiolite, *Earth Planet. Sci. Lett.*, *304*(3–4), 313–325, doi:10.1016/j.epsl.2011.01.029.

Boudier, F., G. Ceuleneer, and A. Nicolas (1988), Shear zones, thrusts and related magmatism in the Oman ophiolite: Initiation of thrusting on an oceanic ridge, *Tectonophysics*, *151*(1–4), 275–296, doi:10.1016/0040-1951(88)90249-1.

Boudier, F., A. Nicolas, B. Ildefonse, and D. Jousselin (1997), EPR microplates, a model for the Oman Ophiolite, *Terra Nova*, *9*(2), 79–82, doi:10.1111/j.1365-3121.1997.tb00007.x.

Bowring, J. F., N. M. McLean, and S. A. Bowring (2011), Engineering cyber infrastructure for U-Pb geochronology: Tripoli and U-Pb_Redux, *Geochem. Geophys. Geosyst.*, *12*, Q0AA19, doi:10.1029/2010GC003479.

Braun, M. G. (2004), Petrologic and microstructural constraints on focused melt transport in dunites and the rheology of the shallow mantle, PhD thesis, 212 pp., MIT-WHOI Joint Program, Cambridge, Mass.

Braun, M. G., G. Hirth, and E. M. Parmentier (2000), The effects of deep damp melting on mantle flow and melt generation beneath mid-ocean ridges, *Earth Planet. Sci. Lett.*, *176*(3–4), 339–356, doi:10.1016/S0012-821X(00)00015-7.

Browning, P., and J. D. Smewing (1981), Processes in magma chambers beneath spreading axes: Evidence from magmatic associations in the Oman Ophiolite, *J. Geol. Soc.*, *138*(3), 279–280, doi:10.1144/gsjgs.138.3.0279.

Ceuleneer, G., A. Nicolas, and F. Boudier (1988), Mantle flow patterns at an oceanic spreading centre: The Oman peridotites record, *Tectonophysics*, *151*(1–4), 1–26, doi:10.1016/0040-1951(88)90238-7.

Ceuleneer, G., M. Monnereau, and I. Amri (1996), Thermal structure of a fossil mantle diapir inferred from the distribution of mafic cumulates, *Nature*, *379*(6561), 149–153, doi:10.1038/379149a0.

de Gramont, X., J. Le Métour, and M. Villey (1986), Samad geologic map, sheet NF40-7C, Minist. of Commer. and Ind., Direct. Gen. of Miner., Muscat.

Dewey, J. F., and J. F. Casey (2011), The origin of obducted large-slab ophiolite complexes, in *Arc-Continent Collision*, edited by D. Brown and P. Ryan, pp. 431–444, Springer, Berlin, doi:10.1007/978-3-540-88558-0_15.

El Amin, O., T. Peters, I. Blechschmidt, M. Al-Battashi, N. Al-Khumasani, and A. Al-Towaya (2005), Ibra geologic map, sheet NF40-8A, Minist. of Commer. and Ind., Direct. Gen. of Miner., Muscat.

France, L., B. Ildefonse, and J. Koepke (2009), Interactions between magma and hydrothermal system in Oman ophiolite and in IODP Hole 1256D: Fossilization of a dynamic melt lens at fast spreading ridges, *Geochem. Geophys. Geosyst.*, *10*, Q10O19, doi:10.1029/2009GC002652.

Garrido, C. J., P. B. Kelemen, and G. Hirth (2001), Variation of cooling rate with depth in lower crust formed at an oceanic spreading ridge: Plagioclase crystal size distributions in gabbros from the Oman ophiolite, *Geochem. Geophys. Geosyst.*, *2*(10), 1041, doi:10.1029/2000GC000136.

Girardeau, J., C. Monnier, L. Lemée, and F. Quatrevaux (2002a), The Wuqbah peridotite, central Oman Ophiolite: Petrological characteristics of the mantle in a fossil overlapping ridge setting, *Mar. Geophys. Res.*, *23*(1), 43–56, doi:10.1023/A:1021297614067.

Girardeau, J., C. Monnier, P. Launeau, and F. Quatrevaux (2002b), Kinematics of mantle flow beneath a fossil overlapping spreading center: The Wuqbah massif case, Oman ophiolite, *Geochem. Geophys. Geosyst.*, *3*(7), 1043, doi:10.1029/2001GC000228.

Gnos, E., and T. Peters (1993), K-Ar ages of the metamorphic sole of the Semail Ophiolite: Implications for ophiolite cooling history, *Contrib. Mineral. Petrol.*, *113*(3), 325–332, doi:10.1007/BF00286925.

Godard, M., D. Jousselin, and J. L. Bodinier (2000), Relationships between geochemistry and structure beneath a palaeo-spreading centre: A study of the mantle section in the Oman ophiolite, *Earth Planet. Sci. Lett.*, *180*(1–2), 133–148, doi:10.1016/S0012-821X(00)00149-7.

Godard, M., J. M. Dautria, and M. Perrin (2003), Geochemical variability of the Oman ophiolite lavas: Relationship with spatial distribution and paleomagnetic directions, *Geochem. Geophys. Geosyst.*, *4*(6), 8609, doi:10.1029/2002GC000452.

Godard, M., D. Bosch, and F. Einaudi (2006), A MORB source for low-Ti magmatism in the Semail ophiolite, *Chem. Geol.*, *234*(1–2), 58–78, doi:10.1016/j.chemgeo.2006.04.005.

Goodenough, K., M. Styles, D. Schofield, R. Thomas, Q. Crowley, R. Lilly, J. McKervey, D. Stephenson, and J. Carney (2010), Architecture of the Oman–UAE ophiolite: Evidence for a multi-phase magmatic history, *Arabian J. Geosci.*, *3*(4), 439–458, doi:10.1007/s12517-010-0177-3.

Gray, D. R., and R. T. Gregory (2000), Implications of the structure of the Wadi Tayin metamorphic sole, the Ibra-Dasir block of the Samail ophiolite, and the Saih Hatat window for late stage extensional ophiolite emplacement, Oman, *Mar. Geophys. Res.*, *21*(3–4), 211–227, doi:10.1023/A:1026772717865.

Gregory, R. T., and H. P. Taylor Jr. (1981), An oxygen isotope profile in a section of Cretaceous oceanic crust, Samail ophiolite, Oman: Evidence for $\delta^{18}O$ buffering of the oceans by deep (>5 km) seawater-hydrothermal circulation at mid-ocean ridges, *J. Geophys. Res.*, *86*(B4), 2737–2755, doi:10.1029/JB086iB04p02737.

Gregory, R. T., D. R. Gray, and J. Miller (1998), Tectonics of the Arabian margin associated with the formation and exhumation of high-pressure rocks, Sultanate of Oman, *Tectonics*, *17*(5), 657–670, doi:10.1029/98TC02206.

Grimes, C. B., B. E. John, M. J. Cheadle, and J. L. Wooden (2008), Protracted construction of gabbroic crust at a slow spreading ridge: Constraints from $^{206}Pb/^{238}U$ zircon ages from Atlantis Massif and IODP Hole U1309D (30°N, MAR), *Geochem. Geophys. Geosyst.*, *9*, Q08012, doi:10.1029/2008GC002063.

Hacker, B. R. (1991), The role of deformation in the formation of metamorphic gradients: Ridge subduction beneath the Oman Ophiolite, *Tectonics*, *10*(2), 455–473, doi:10.1029/90TC02779.

Hacker, B. R. (1994), Rapid emplacement of young oceanic lithosphere: Argon geochronology of the Oman Ophiolite, *Science*, *265*(5178), 1563–1565, doi:10.1126/science.265.5178.1563.

Hacker, B. R., J. L. Mosenfelder, and E. Gnos (1996), Rapid emplacement of the Oman ophiolite: Thermal and geochronologic constraints, *Tectonics*, *15*(6), 1230–1247, doi:10.1029/96TC01973.

Hanghøj, K., P. B. Kelemen, D. Hassler, and M. Godard (2010), Composition and genesis of depleted mantle peridotites from the Wadi Tayin massif, Oman ophiolite; Major and trace element geochemistry, and Os isotope and PGE systematics, *J. Petrol.*, *51*(1–2), 201–227, doi:10.1093/petrology/egp077.

Harrison, T., and E. Watson (1983), Kinetics of zircon dissolution and zirconium diffusion in granitic melts of variable water content, *Contrib. Mineral. Petrol.*, *84*(1), 66–72, doi:10.1007/BF01132331.

Hofmann, A. W. (2007), Sampling mantle heterogeneity through oceanic basalts: Isotopes and trace elements, in *Treatise on Geochemistry*, vol. 2, *The Mantle and Core*, edited by D. H. Heinrich and K. T. Karl, pp. 1–44, Pergamon, Oxford, U. K., doi:10.1016/B0-08-043751-6/02123-X.

Homburg, J. M., G. Hirth, and P. B. Kelemen (2010), Investigation of the strength contrast at the Moho: A case study from the Oman Ophiolite, *Geology*, *38*(8), 679–682, doi:10.1130/G30880.1.

Hopson, C. A., R. G. Coleman, R. T. Gregory, J. S. Pallister, and E. H. Bailey (1981), Geologic section through the Samail ophiolite and associated rocks along a Muscat-Ibra transect, southeastern Oman Mountains, *J. Geophys. Res.*, *86*(B4), 2527–2544, doi:10.1029/JB086iB04p02527.

Ildefonse, B., A. Nicolas, and F. Boudier (1993), Evidence from the Oman ophiolite for sudden stress changes during melt injection at oceanic spreading centres, *Nature*, *366*(6456), 673–675, doi:10.1038/366673a0.

Jaffey, A. H., K. F. Flynn, L. E. Glendenin, W. C. Bentley, and A. M. Essling (1971), Precision measurement of half-lives and specific activities of ^{235}U and ^{238}U, *Phys. Rev. C*, *4*(5), 1889–1906, doi:10.1103/PhysRevC.4.1889.

Jousselin, D., and A. Nicolas (2000), Oceanic ridge off-axis deep structure in the Mansah region (Sumail massif, Oman ophiolite), *Mar. Geophys. Res.*, *21*(3–4), 243–257, doi:10.1023/A:1026741208295.

Juteau, T., M. Ernewein, I. Reuber, H. Whitechurch, and R. Dahl (1988), Duality of magmatism in the plutonic sequence of the Sumail Nappe, Oman, *Tectonophysics*, *151*(1–4), 107–135, doi:10.1016/0040-1951(88)90243-0.

Kelemen, P. B., and E. Aharonov (1998), Periodic formation of magma fractures and generation of layered gabbros in the lower crust beneath oceanic spreading ridges, in *Faulting and Magmatism at Mid-Ocean Ridges*, *Geophys. Monogr. Ser.*, vol. 106, edited by W. Roger Buck et al., pp. 267–289, AGU, Washington, D. C., doi:10.1029/GM106p0267.

Kelemen, P. B., K. Koga, and N. Shimizu (1997a), Geochemistry of gabbro sills in the crust-mantle transition zone of the Oman ophiolite: Implications for the origin of the oceanic lower crust, *Earth Planet. Sci. Lett.*, *146*(3–4), 475–488, doi:10.1016/S0012-821X(96)00235-X.

Kelemen, P. B., G. Hirth, N. Shimizu, M. Spiegelman, and H. J. B. Dick (1997b), A review of melt migration processes in the adiabatically upwelling mantle beneath oceanic spreading ridges, *Philos. Trans. Math. Phys. Eng. Sci.*, *355*(1723), 283–318.

Koepke, J., S. T. Feig, J. Snow, and M. Freise (2004), Petrogenesis of oceanic plagiogranites by partial melting of gabbros: An experimental study, *Contrib. Mineral. Petrol.*, *146*(4), 414–432, doi:10.1007/s00410-003-0511-9.

Kuiper, K. F., A. Deino, F. J. Hilgen, W. Krijgsman, P. R. Renne, and J. R. Wijbrans (2008), Synchronizing rock clocks of Earth history, *Science*, *320*(5875), 500–504, doi:10.1126/science.1154339.

Lanphere, M. A. (1981), K-Ar ages of metamorphic rocks at the base of the Samail ophiolite, Oman, *J. Geophys. Res.*, *86*(B4), 2777–2782, doi:10.1029/JB086iB04p02777.

Lippard, S. J., A. W. Shelton, and I. G. Gass (1986), *The Ophiolite of Northern Oman*, 178 pp., Geol. Soc., London.

Lissenberg, C. J., M. Rioux, N. Shimizu, S. A. Bowring, and C. Mevel (2009), Zircon dating of oceanic crustal accretion, *Science*, *323*(5917), 1048–1050, doi:10.1126/science.1167330.

Luyendyk, B. P., and R. Day (1982), Paleomagnatism of the Samail ophiolite, Oman: 2. The Wadi Kadir gabbro section, *J. Geophys. Res.*, *87*(B13), 10,903–10,917, doi:10.1029/JB087iB13p10903.

Luyendyk, B. P., B. R. Laws, R. Day, and T. B. Collinson (1982), Paleomagnatism of the Samail ophiolite, Oman: 1. The sheeted dike complex at Ibra, *J. Geophys. Res.*, *87*(B13), 10,883–10,902, doi:10.1029/JB087iB13p10883.

MacLeod, C. J., and D. A. Rothery (1992), Ridge axial segmentation in the Oman ophiolite: Evidence from along-strike variations in the sheeted dyke complex, *Geol. Soc. London Spec. Publ.*, *60*(1), 39–63, doi:10.1144/GSL.SP.1992.060.01.03.

MacLeod, C. J., and G. Yaouancq (2000), A fossil melt lens in the Oman ophiolite: Implications for magma chamber processes at fast spreading ridges, *Earth Planet. Sci. Lett.*, *176*(3–4), 357–373, doi:10.1016/S0012-821X(00)00020-0.

MacLeod, C. J., C. J. Lissenberg, L. E. Bibby, J. A. Pearce, K. M. Goodenough, M. T. Styles, and D. J. Condon (2012), Geodynamic setting and origin of the Oman/UAE ophiolite, paper presented at International Conference on the Geology of the Arabian Plate and the Oman Mountains, Sultan Qaboos Univ., Muscat, Sultanate of Oman, 7–9 Jan.

Mattinson, J. M. (2005), Zircon U/Pb chemical abrasion (CA-TIMS) method: Combined annealing and multi-step partial dissolution analysis for improved precision and accuracy of zircon ages, *Chem. Geol.*, *220*(1–2), 47–66, doi:10.1016/j.chemgeo.2005.03.011.

McCulloch, M. T., R. T. Gregory, G. J. Wasserburg, and H. P. Taylor (1981), Sm-Nd, Rb-Sr, and ^{18}O/^{16}O isotopic systematics in an oceanic crustal section: Evidence from the Samail Ophiolite, *J. Geophys. Res.*, *86*(B4), 2721–2735, doi:10.1029/JB086iB04p02721.

McLean, N. M., J. F. Bowring, and S. A. Bowring (2011), An algorithm for U-Pb isotope dilution data reduction and uncertainty propagation, *Geochem. Geophys. Geosyst.*, *12*, Q0AA18, doi:10.1029/2010GC003478.

Min, K., R. Mundil, P. R. Renne, and K. R. Ludwig (2000), A test for systematic errors in ^{40}Ar/^{39}Ar geochronology through comparison with U/Pb analysis of a 1.1-Ga rhyolite, *Geochim. Cosmochim. Acta*, *64*(1), 73–98, doi:10.1016/S0016-7037(99)00204-5.

Miyashita, S., Y. Adachi, and S. Umino (2003), Along-axis magmatic system in the northern Oman ophiolite: Implications of compositional variation of the sheeted dike complex, *Geochem. Geophys. Geosyst.*, *4*(9), 8617, doi:10.1029/2001GC000235.

Montigny, R., O. Le Mer, R. Thuizat, and H. Whitechurch (1988), K-Ar and Ar study of metamorphic rocks associated with the Oman ophiolite: Tectonic implications, *Tectonophysics*, *151*(1–4), 345–362.

Nicolas, A. (1989), *Structures of Ophiolites and Dynamics of Oceanic Lithosphere*, 367 pp., Kluwer Acad., London, doi:10.1007/978-94-009-2374-4.

Nicolas, A., and F. Boudier (1995), Mapping oceanic ridge segments in Oman ophiolite, *J. Geophys. Res.*, *100*(B4), 6179–6197, doi:10.1029/94JB01188.

Nicolas, A., and F. Boudier (2003), Where ophiolites come from and what they tell us, *Spec. Pap. Geol. Soc. Am.*, *373*, 137–152.

Nicolas, A., and F. Boudier (2008), Large shear zones with no relative displacement, *Terra Nova*, *20*(3), 200–205, doi:10.1111/j.1365-3121.2008.00806.x.

Nicolas, A., and F. Boudier (2011), Structure and dynamics of ridge axial melt lenses in the Oman ophiolite, *J. Geophys. Res.*, *116*, B03103, doi:10.1029/2010JB007934.

Nicolas, A., I. Reuber, and K. Benn (1988), A new magma chamber model based on structural studies in the Oman ophiolite, *Tectonophysics*, *151*(1–4), 87–105, doi:10.1016/0040-1951(88)90242-9.

Nicolas, A., F. Boudier, and B. Ildefonse (1996), Variable crustal thickness in the Oman ophiolite: Implication for oceanic crust, *J. Geophys. Res.*, *101*(B8), 17,941–17,950, doi:10.1029/96JB00195.

Nicolas, A., F. Boudier, B. Ildefonse, and E. Ball (2000a), Accretion of Oman and United Arab Emirates ophiolite—Discussion of a new structural map, *Mar. Geophys. Res.*, *21*(3–4), 147–180, doi:10.1023/A:1026769727917.

Nicolas, A., B. Ildefonse, F. Boudier, X. Lenoir, and W. Ben Ismail (2000b), Dike distribution in the Oman-United Arab Emirates ophiolite, *Mar. Geophys. Res.*, *21*(3–4), 269–287, doi:10.1023/A:1026718026951.

Nicolas, A., F. Boudier, J. Koepke, L. France, B. Ildefonse, and C. Mevel (2008), Root zone of the sheeted dike complex in the Oman ophiolite, *Geochem. Geophys. Geosyst.*, *9*, Q05001, doi:10.1029/2007GC001918.

Nicolas, A., F. Boudier, and L. France (2009), Subsidence in magma chamber and the development of magmatic foliation in Oman ophiolite gabbros, *Earth Planet. Sci. Lett.*, *284*(1–2), 76–87, doi:10.1016/j.epsl.2009.04.012.

Pallister, J. S. (1981), Structure of the sheeted dike complex of the Samail ophiolite near Ibra, Oman, *J. Geophys. Res.*, *86*(B4), 2661–2672, doi:10.1029/JB086iB04p02661.

Pallister, J. S., and C. A. Hopson (1981), Samail ophiolite plutonic suite: Field relations, phase variation, cryptic variation and layering, and a model of a spreading ridge magma chamber, *J. Geophys. Res.*, *86*(B4), 2593–2644, doi:10.1029/JB086iB04p02593.

Pallister, J. S., and R. J. Knight (1981), Rare-earth element geochemistry of the Samail ophiolite near Ibra, Oman, *J. Geophys. Res.*, *86*(B4), 2673–2697, doi:10.1029/JB086iB04p02673.

Peacock, S. M. (1990), Numerical simulation of metamorphic pressure-temperature-time paths and fluid production in subducting slabs, *Tectonics*, *9*(5), 1197–1211, doi:10.1029/TC009i005p01197.

Pearce, J. A., T. Alabaster, A. W. Shelton, and M. P. Searle (1981), The Oman ophiolite as a Cretaceous arc-basin complex: Evidence and implications, *Philos. Trans. R. Soc. London, Ser. A*, *300*(1454), 299–317, doi:10.1098/rsta.1981.0066.

Perrin, M., M. Prevot, and F. Bruere (1994), Rotation of the Oman ophiolite and initial location of the ridge in the hotspot reference frame, *Tectonophysics*, *229*(1–2), 31–42, doi:10.1016/0040-1951(94)90004-3.

Perrin, M., G. Plenier, J.-M. Dautria, E. Cocuaud, and M. Prévot (2000), Rotation of the Semail ophiolite (Oman): Additional paleomagnetic data from the volcanic sequence, *Mar. Geophys. Res.*, *21*(3–4), 181–194, doi:10.1023/A:1026738313805.

Python, M., and G. Ceuleneer (2003), Nature and distribution of dykes and related melt migration structures in the mantle section of the Oman ophiolite, *Geochem. Geophys. Geosyst.*, *4*(7), 8612, doi:10.1029/2002GC000354.

Reid, I., and H. R. Jackson (1981), Oceanic spreading rate and crustal thickness, *Mar. Geophys. Res.*, *5*(2), 165–172.

Renne, P. R., C. C. Swisher, A. L. Deino, D. B. Karner, T. L. Owens, and D. J. DePaolo (1998), Intercalibration of standards, absolute ages and uncertainties in $^{40}Ar/^{39}Ar$ dating, *Chem. Geol.*, *145*(1–2), 117–152, doi:10.1016/S0009-2541(97)00159-9.

Reuber, I., P. Nehlig, and T. Juteau (1991), Axial segmentation at a fossil oceanic spreading centre in the Haylayn block (Semail nappe, Oman): Off-axis mantle diapir and advancing ridge tip, *J. Geodyn.*, *13*(2–4), 253–278, doi:10.1016/0264-3707(91)90041-C.

Rioux, M., C. J. Lissenberg, N. M. McLean, S. A. Bowring, C. J. MacLeod, E. Hellebrand, and N. Shimizu (2012), Protracted timescales of lower crustal growth at the fast-spreading East Pacific Rise, *Nat. Geosci.*, *5*, 275–278, doi:10.1038/ngeo1378.

Rollinson, H. (2009), New models for the genesis of plagiogranites in the Oman ophiolite, *Lithos*, *112*(3–4), 603–614, doi:10.1016/j.lithos.2009.06.006.

Schwartz, J. J., B. E. John, M. J. Cheadle, E. A. Miranda, C. B. Grimes, J. L. Wooden, and H. J. B. Dick (2005), Dating the growth of oceanic crust at a slow-spreading ridge, *Science*, *310*(5748), 654–657, doi:10.1126/science.1116349.

Searle, M., and J. Cox (1999), Tectonic setting, origin, and obduction of the Oman ophiolite, *Geol. Soc. Am. Bull.*, *111*(1), 104–122, doi:10.1130/0016-7606(1999)111<0104:TSOAOO>2.3.CO;2.

Searle, M., and J. Cox (2002), Subduction zone metamorphism during formation and emplacement of the Semail ophiolite in the Oman Mountains, *Geol. Mag.*, *139*(3), 241–255, doi:10.1017/S0016756802006532.

Searle, M. P., and J. Malpas (1980), The structure and metamorphism of rocks beneath the Semail Ophiolite of Oman and their significance in ophiolite obduction, *Trans. R. Soc. Edinburgh Earth Sci.*, *71*, 247–262, doi:10.1017/S0263593300013614.

Searle, M. P., S. J. Lippard, J. D. Smewing, and D. C. Rex (1980), Volcanic rocks beneath the Semail Ophiolite nappe in the northern Oman mountains and their significance in the Mesozoic evolution of Tethys, *J. Geol. Soc.*, *137*(5), 589–604, doi:10.1144/gsjgs.137.5.0589.

Sleep, N. H. (1975), Formation of oceanic crust: Some thermal constraints, *J. Geophys. Res.*, *80*(29), 4037–4042, doi:10.1029/JB080i029p04037.

Smewing, J. D. (1981), Mixing characteristics and compositional differences in mantle-derived melts beneath spreading axes: Evidence from cyclically layered rocks in the ophiolite of North Oman, *J. Geophys. Res.*, *86*(B4), 2645–2659, doi:10.1029/JB086iB04p02645.

Stakes, D. S., and H. P. Taylor (2003), Oxygen isotope and chemical studies on the origin of large plagiogranite bodies in northern Oman, and their relationship to the overlying massive sulphide deposits, *Geol. Soc. London Spec. Publ.*, *218*(1), 315–351, doi:10.1144/GSL.SP.2003.218.01.17.

Tamura, A., and S. Arai (2006), Harzburgite-dunite-orthopyroxenite suite as a record of supra-subduction zone setting for the Oman ophiolite mantle, *Lithos*, *90*(1–2), 43–56, doi:10.1016/j.lithos.2005.12.012.

Tilton, G. R., C. A. Hopson, and J. E. Wright (1981), Uranium-lead isotopic ages of the Samail ophiolite, Oman, with applications to Tethyan ocean ridge tectonics, *J. Geophys. Res.*, *86*(B4), 2763–2775, doi:10.1029/JB086iB04p02763.

VanTongeren, J. A., P. B. Kelemen, and K. Hanghøj (2008), Cooling rates in the lower crust of the Oman ophiolite: Ca in olivine, revisited, *Earth Planet. Sci. Lett.*, *267*(1–2), 69–82, doi:10.1016/j.epsl.2007.11.034.

Warren, C., R. Parrish, D. Waters, and M. Searle (2005), Dating the geologic history of Oman's Semail ophiolite: Insights from U-Pb geochronology, *Contrib. Mineral. Petrol.*, *150*(4), 403–422, doi:10.1007/s00410-005-0028-5.

Weiler, P. D. (2000), Differential rotations in the Oman Ophiolite: Paleomagnetic evidence from the southern massifs, *Mar. Geophys. Res.*, *21*(3–4), 195–210, doi:10.1023/A:1026760331977.

Wendt, I., and C. Carl (1991), The statistical distribution of the mean squared weighted deviation, *Chem. Geol.*, *86*(4), 275–285.